AD NUMBER

AD812070

LIMITATION CHANGES

TO:

Approved for public release; distribution is unlimited.

FROM:

Distribution authorized to U.S. Gov't. agencies and their contractors; Critical Technology; DEC 1966. Other requests shall be referred to Army Ballistic Research Laboratories, Aberdeen Proving Ground, MD 21005. This document contains export-controlled technical data.

AUTHORITY

USAARADCOM ltr, 20 Feb 1981

BRL

AD

REPORT NO. 1350

SHOCK CURVATURE AND GRADIENTS AT THE TIP OF POINTED AXISYMMETRIC BODIES IN NONEQUILIBRIUM FLOW

by

R. Sedney
N. Gerber

December 1966

U. S. ARMY MATERIEL COMMAND
BALLISTIC RESEARCH LABORATORIES
ABERDEEN PROVING GROUND, MARYLAND

Destroy this report when it is no longer needed.
Do not return it to the originator.

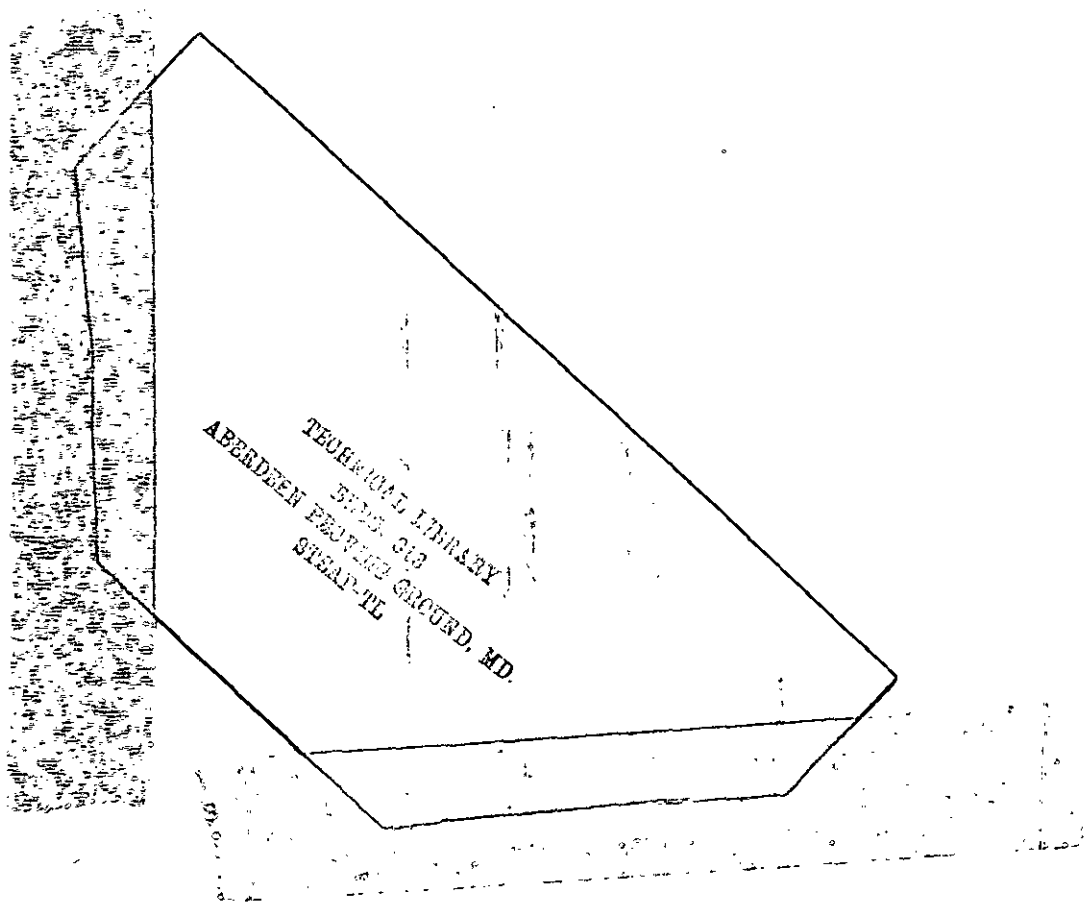

The findings in this report are not to be construed as an official Department of the Army position, unless so designated by other authorized documents.

B A L L I S T I C R E S E A R C H L A B O R A T O R I E S

REPORT NO. 1350

DECEMBER 1966

SHOCK CURVATURE AND GRADIENTS AT THE TIP OF POINTED AXISYMMETRIC BODIES IN NONEQUILIBRIUM FLOW

R. Sedney
N. Gerber

Exterior Ballistics Laboratory

RDT&E Project No. 1P222901A201

A B E R D E E N P R O V I N G G R O U N D, M A R Y L A N D

B A L L I S T I C R E S E A R C H L A B O R A T O R I E S

REPORT NO. 1350

RSedney/NGerber/sjw
Aberdeen Proving Ground, Md.
December 1966

SHOCK CURVATURE AND GRADIENTS AT THE TIP OF POINTED AXISYMMETRIC BODIES IN NONEQUILIBRIUM FLOW

ABSTRACT

The shock curvature and flow variable gradients at the tip of a pointed body caused by nonequilibrium effects are considered. Coordinates introduced by Chester are used since they offer a convenient way of treating the boundary conditions. The desired functions are obtained by solving numerically a system of linear ordinary differential equations. These equations have a singularity; the nature of the singularity is found analytically, and its numerical treatment is discussed. The specific nonequilibrium effect considered is vibrational relaxation in a pure diatomic gas. Representative results are given for flow of N_2 over a cone for a comprehensive range of Mach number and cone angle. There is a point analogous to the Crocco point. These results compare favorably with those obtained by South and Newman using an approximate method. Another check is made by comparison with characteristic calculations extrapolated to the origin.

TABLE OF CONTENTS

LIST OF SYMBOLS

b, f, g, j — functions defined in equation (3.4)

c'_{p_a} — specific heat at const. pres. (translat. and rotat. modes)

c'_{v_a} — specific heat at const. vol. (translat., and rotat. modes)

h'_t — total enthalpy per unit mass $h_t = h_t'/[c'_{p_a} T_\infty']$

p' — pressure $p = p'/p_\infty'$

q' — speed of flow $q = q'/q_\infty'$

s' — arc length along streamline $s = s'/[\tau_b' q_\infty']$

u' — velocity component in x' direction $u = u''/q_\infty'$

v' — velocity component in y' direction $v = v'/q_\infty'$

x' — coordinate parallel to axis of symmetry $x = x'/[\tau_b' q_\infty']$

y' — coordinate normal to axis of symmetry $y = y'/[\tau_b' q_\infty']$

A, B, C, F, G — functions defined in equation (3.5)

c' — constant occurring in expression for τ $c = c'/T_\infty'$

D — function defined in equation (2.13)

E' — vibrational energy per unit mass $E = E'/[c'_{p_a} T_\infty']$

$\overset{*}{E}'(T')$ — equilib. vibrat. energy per unit mass at temp. T'

$\overset{*}{E} = \overset{*}{E}'/(c'_{p_a} T_\infty')$

K_b — body curvature at tip

K_w — shock wave curvature at tip

M — local Mach number

LIST OF SYMBOLS (Contd)

P — $(\partial p/\partial \eta)_{\eta} = 0$

R — $(\partial \rho/\partial \eta)_{\eta} = 0$

T' — temperature $T = T'/T_{\infty}'$

U — $(\partial u/\partial \eta)_{\eta} = 0$

V — $(\partial v/\partial \eta)_{\eta} = 0$

Z — Θ_{v}'/T_{∞}'

β — angle between x' axis and tangent to shock wave

γ — c'_{p_a}/c'_{v_a} = 1.4 in present calculations

ϵ — 0 for ideal gas flow, = 1 for nonequilib. flow

ζ — Chester variable $\zeta = 2\psi'/[\rho_{\infty}' q_{\infty}' y'^{2}]$

η — Chester variable $\eta = y$

θ — angle between velocity vector and x' axis

Θ_{v}' — characteristic vibrational temperature of the gas

ρ' — density $\rho = \rho'/\rho_{\infty}'$

τ' — relaxation time $\tau = \tau'/\tau_{b}'$

ψ' — stream function

Φ — function defined in equation (2.6)

Ω — $(\partial E/\partial \eta)_{\eta} = 0$

Subscripts

∞	– free stream conditions
b	– body
w	– shock wave
h	– refers to homogeneous differential equations and their solution
n	– refers to particular solution to nonhomogeneous differential equations

Superscript

$'$	– denotes quantity with dimensions

1. INTRODUCTION

When nonequilibrium effects are considered in the fluid dynamic equations, the classical similar solutions describing supersonic flow over wedges and cones no longer exist. To gain some insight into nonequilibrium effects one can seek solutions valid in restricted regions of a flow, e.g., the vicinity of the tip of a wedge or cone. The first approximation to the flow here is the frozen (similar) solution. The next approximation brings into evidence the nonequilibrium effects, such as the curvature of the shock wave. The purpose of this work is to find this approximation for the case of flow over a cone and pointed ogives in general.

The corresponding problem for wedge flow (Sedney, 1961) is resolved by explicit solution of algebraic equations. For cone flow, differential equations with two-point boundary conditions (at shock and body surface) must be solved. The coefficients of these equations, which involve the frozen conical flow solution, give rise to a singular point, at least in all choices of coordinates investigated.

There is a close analogy between the problem of approximating the nonequilibrium flow in the neighborhood of the tip of a wedge or cone and that of approximating the equilibrium or frozen flow near the tip of a pointed-ogive body. The latter problem was solved by Crocco (1937) for two dimensional flow and by Shen and Lin (1951) for axisymmetric flow. In order to treat the singularity for the axisymmetric case, and especially its effects on higher approximations, Kogan (1956) formulated the problem in terms of Crocco's stream function. This refinement, however, is not included in the values of shock curvature hitherto published, Shen and Lin (1951), and Bianco et al, (1960).

In the method of solution adopted here for determining shock curvature and gradients caused by nonequilibrium effects, these same quantities for frozen flow over ogival bodies are obtained as a by-product. The specific source of the nonequilibrium effects considered here is vibrational relaxation of a diatomic gas; however, the present

method can be employed for dissociation, ionization, etc. The model of a vibrationally excited gas serves as well as any other example to illustrate the technique and effects.

A distinctive feature of this analysis is the choice of coordinates. Specifically the coordinates used are those introduced by Chester (1956) in his study of hypersonic flow over blunt bodies. The chief advantage of this choice is the ease of handling the boundary conditions on the shock; for here the unknown shock curve is mapped into one of the coordinate lines. Also the singular point at the tip is spread out into a line interval along the second coordinate axis. The latter, but not the former, advantage is also gained with polar coordinates. The differential equations now have an integrable, inverse one-half power-type of singularity at the origin. This could be handled in the standard way -- using expansions to match the numerical solution; instead the entire problem is treated numerically, the authors believe this procedure to be more efficient. The singularity is treated by a "detailed approach to the body" which involves decreasing the step size in the Runge-Kutta numerical integration procedure.

The motivation for this work arose in the computation of nonequilibrium flows over cones, Sedney and Gerber (1963), by the method of characteristics. One is forced to initiate that calculation by assuming a finite frozen flow region. The effect of this error can be relatively large and propagate two or three lengths of the original frozen region downstream even though the grid size is twenty to thirty times less than this length. The behavior near the tip can be studied by the laborious process of choosing successively smaller frozen flow regions.

The results of the present paper can be used as a check on those from the characteristic method. Alternatively, they can be used as input to start the characteristic calculation. With the improved approximation to the flow near the tip, a larger grid size is possible and a saving on computation time realized.

2. FLOW EQUATIONS

The axisymmetric flows to be considered are steady, inviscid, and isoenergetic. The equations for conservation of mass, momentum, and energy are, in non-dimensional form,

$$\frac{\partial}{\partial x}(y\rho u) + \frac{\partial}{\partial y}(y\rho v) = 0 \tag{2.1}$$

$$\gamma M_\infty^2 \left[u\frac{\partial u}{\partial x} + v\frac{\partial u}{\partial y}\right] = -\frac{1}{\rho}\frac{\partial p}{\partial x} \tag{2.2}$$

$$\gamma M_\infty^2 \left[u\frac{\partial v}{\partial x} + v\frac{\partial v}{\partial y}\right] = -\frac{1}{\rho}\frac{\partial p}{\partial y} \tag{2.3}$$

$$\frac{\gamma-1}{2} M_\infty^2 (u^2 + v^2) + T + E = h_t \tag{2.4}$$

See *Figure 1 for notation* (*where primes indicate dimensional quantities*); ρ is density, p is pressure, T is temperature, E is vibrational energy per unit mass, γ is the ratio of frozen specific heats, and h_t is the constant total enthalpy. Variables are made dimensionless as follows: lengths by $\tau_b' q_\infty'$ where τ_b' is the relaxation time evaluated at the frozen conditions on the body tip and q_∞' is free stream velocity; velocities, pressure, density, and temperature by their free stream values; vibrational energy by $c_{pa}' T_\infty'$, the frozen enthalpy in the free stream. The model chosen for the diatomic gas with vibrational relaxation is discussed in Sedney (1961). The perfect gas law is assumed

$$p = \rho T \tag{2.5}$$

and the rate equation is

$$u\frac{\partial E}{\partial x} + v\frac{\partial E}{\partial y} = [E^*(T) - E]/\tau \equiv \Phi \tag{2.6}$$

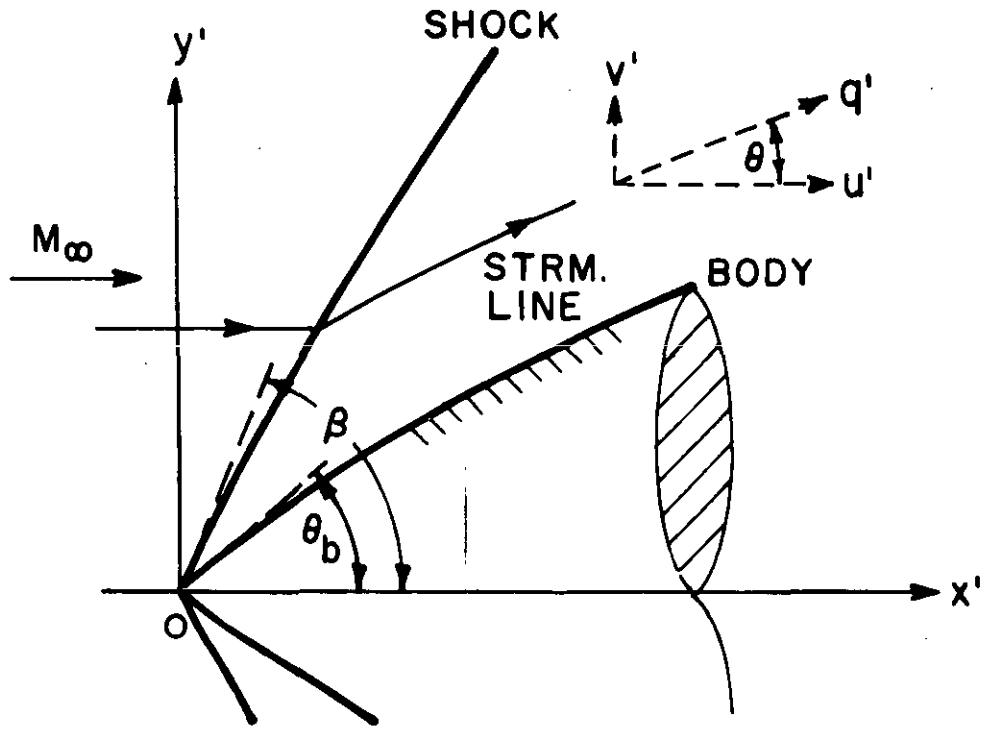

Figure 1. Cross-sectional view of flow field in the physical plane. (q′ = flow speed; u′, v′ = velocity components in coordinate directions.)

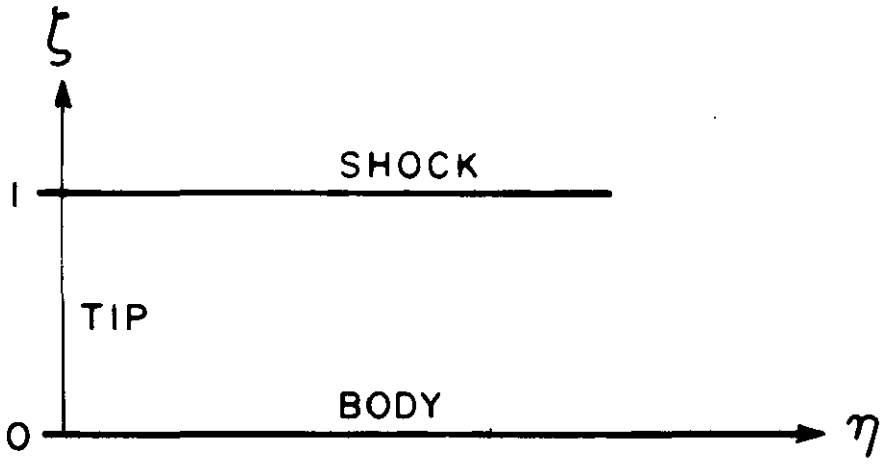

Figure 2. Flow region in the ζ, η plane.

where τ is the relaxation time referred to τ_b', and $E^*(T)$ is the local equilibrium value of E, given by

$$E^*(T) = (2Z/7)/(e^{Z/T} - 1)$$

with $Z = \Theta_v'/T_\infty'$, Θ_v' = characteristic vibrational temperature. The variation of τ with T and p is approximated by

$$\tau = (p_b/p) \exp [(c/T)^{1/3} - (c/T_b)^{1/3}]$$

and the subscript b refers to conditions on the body at the tip. The constant c is evaluated for various temperature ranges by fitting experimental data; e.g., those of Blackman (1956) or Millikan and White (1963).

The independent variables x,y are transformed to ζ, η by

$$\zeta = 2\psi(x,y)/y^2, \quad \eta = y \tag{2.7}$$

where ψ is the dimensionless stream function

$$\partial\psi/\partial x = -y\rho v, \quad \partial\psi/\partial y = y\rho u$$

Thus $\frac{\partial}{\partial x} = -\frac{2\rho v}{\eta}\frac{\partial}{\partial \zeta}$ and $\frac{\partial}{\partial y} = \frac{\partial}{\partial \eta} + \frac{2(\rho u - \zeta)}{\eta}\frac{\partial}{\partial \zeta}$; and Equations (2.1), (2.2), (2.3), and (2.6) become, respectively,

$$2\frac{\partial}{\partial \zeta}\left(\frac{u}{v}\right) - 2\frac{\partial}{\partial \zeta}\left(\frac{\zeta}{\rho v}\right) + \frac{\partial}{\partial \eta}\left(\frac{\eta}{\rho v}\right) = 0 \tag{2.8}$$

$$\left(\frac{2}{\gamma M_\infty^2}\right)\frac{\partial p}{\partial \zeta} = \eta\frac{\partial u}{\partial \eta} - 2\zeta\frac{\partial u}{\partial \zeta} \tag{2.9}$$

$$\left(\frac{\gamma M_\infty^2}{2}\right)\left[\eta \frac{\partial}{\partial \eta}(u^2 + v^2) - 2\zeta \frac{\partial}{\partial \zeta}(u^2 + v^2)\right] = -\frac{1}{\rho}\left(\eta \frac{\partial p}{\partial \eta} - 2\zeta \frac{\partial p}{\partial \zeta}\right) \quad (2.10)$$

$$v\left(\eta \frac{\partial E}{\partial \eta} - 2\zeta \frac{\partial E}{\partial \zeta}\right) = \frac{\eta}{\tau}[E^*(T) - E] \quad (2.11)$$

Note that if vibrational energy in the free stream is negligible ($E_\infty = 0$)

$$h_t = 1 + (1/2)(\gamma - 1) M_\infty^2$$

This would be the case if $T_\infty << \Theta_v$ and equilibrium existed in the free stream. If the free stream is out of equilibrium E_∞ will, in general, not be negligible. This would occur if a cone were placed in the test section of a shock tunnel since the free stream is generally frozen in such a facility. In any case, behind the shock, E takes its free stream value.

The variables ζ and η were employed by Chester in the study of hypersonic flow past blunt bodies. In the present problem the shock wave is attached at the pointed tip of the body, but the flow region is mapped into the same strip of the ζ, η plane as for the case of a detached shock. This strip is shown in Figure 2 where it is seen that the tip transforms into the line segment $\eta = 0$, $0 \leq \zeta \leq 1$. This stretching is necessary to examine the singularity at the tip. It is also accomplished by using polar coordinates (when properly plotted on rectangular axes); however, the shock curve is unknown then. The same strip is obtained if a body-oriented coordinate system is used and the normal coordinate is normalized by the total distance between the body and shock.

If the body is a cone and the flow is either frozen or in equilibrium so that the flow is conical, then the flow variables are constant along the lines ζ = constant. This is shown using the fact

that ψ is homogeneous of degree two in the variables x and y, a result which follows from the definition of ψ and the fact that ρu and ρv are homogeneous of degree zero. The streamlines are always the hyperbolae, $\zeta\eta^2$ = constant.

On physical grounds one would expect that the flow at the tip, $\eta = 0$, should be frozen; this is easily proved from Equations (2.8) - (2.11). Setting $\eta = 0$, all terms containing $\partial/\partial\eta$ vanish, $\partial E/\partial\zeta = 0$, and the remaining equations give

$$\frac{du}{d\zeta} = \frac{1}{2}\left(\frac{pv}{\rho^2}\right)/D$$

$$\frac{dv}{d\zeta} = -\frac{1}{2}\left[\frac{p(\rho u - \zeta)}{\rho^3}\right]/D$$

$$\frac{d\rho}{d\zeta} = -\frac{1}{2}\left(\frac{M_\infty^2 \zeta v}{p}\right)/D \qquad (2.12)$$

$$\frac{dp}{d\zeta} = -\frac{1}{2}\left(\frac{\gamma M_\infty^2 pv\zeta}{\rho^2}\right)/D$$

$$D = \frac{p(\rho u - \zeta)^2}{v\rho^3} + \frac{v}{\rho}\left(p - \frac{M_\infty^2 \zeta^2}{\rho}\right) \qquad (2.13)$$

Since $\partial E/\partial\zeta = 0$ along $\eta = 0$, E is then constant there; i.e., the flow is frozen at the tip. The constant will be the free stream value of E.

The Equations (2.12) are those for conical frozen (Taylor-Maccoll) flow in the coordinates ζ, η; their numerical solution is a necessary step in the determination of the gradients since the frozen flow variables appear as coefficients in the gradient equations. This solution is

obtained by integrating from the shock, $\zeta = 1$, to the body, $\zeta = 0$, given M_∞, γ, and β, where tan β is the shock wave slope. The initial conditions at the shock are the standard frozen shock relations:

$$u_w = 1 - \frac{2(M_\infty^2 \sin^2 \beta - 1)}{(\gamma + 1)M_\infty^2} \tag{2.14}$$

and so forth. The half-angle of the body tip is determined from

$$\tan \theta_b = (v/u)_{\zeta = 0} \tag{2.15}$$

One can integrate several cases and then interpolate to find a desired half-angle or set up an iteration procedure to yield this result.

3. GRADIENT EQUATIONS

The equations for the gradients of the flow variables are obtained by differentiating Equations (2.8) - (2.11) with respect to η, then setting η equal to zero. This requires the assumption* that $\partial^2/\partial\zeta\partial\eta = \partial^2/\partial\eta\partial\zeta$.

The following notation is introduced:

$$U = (\partial u/\partial\eta)_{\eta = 0}, \quad V = (\partial v/\partial\eta)_{\eta = 0}, \quad \Omega = (\partial E/\partial\eta)_{\eta = 0}$$
$$R = (\partial\rho/\partial\eta)_{\eta = 0}, \quad P = (\partial p/\partial\eta)_{\eta = 0} \tag{3.1}$$

---

* *The set of mathematical conditions insuring the interchangeability of second derivatives is different from that insuring the validity of an expansion of the form* $f(\eta,\zeta)_b + (\partial f/\partial\eta)_b\eta + O(\eta^2)$. *Neither set can be verified a priori.*

Hereafter, it is understood that all quantities are evaluated at $\eta = 0$. The differential equations for the gradient functions are (where $\dot{} \equiv d/d\zeta$)

$$\dot{\Omega} = (\Omega - \Phi/v)/(2\zeta) \tag{3.2}$$

$$\dot{U} = (1/D)\ [vG/\rho + b\ (C - \varepsilon\Omega)/\zeta] \tag{3.3a}$$

$$\dot{V} = (1/D)\ [-gG/\rho + f\ (C - \varepsilon\Omega)/\zeta] \tag{3.3b}$$

$$\dot{R} = -\ [M_\infty^{\,2}\ v\zeta B + (g^2 + v^2)(A - \varepsilon F)/v + j(C - \varepsilon\Omega)/\zeta]/D \tag{3.3c}$$

where the denominator D is the same as in Equation (2.13). The coefficients g, b, f, and j are known functions of ζ:

$$\begin{aligned} g &= u - \zeta/\rho \\ b &= [pg/v - (\gamma - 1)\ M_\infty^{\,2}\ v\zeta]/(2\gamma\ M_\infty^{\,2}\rho) \\ f &= [\zeta\ M_\infty^{\,2}\ (\gamma g - u) + p]/(2\gamma\ M_\infty^{\,2}\rho) \\ j &= \rho\ [(\gamma - 1)\ v^2 + g\ (\gamma\ g - u)]/(2\gamma\ v), \end{aligned} \tag{3.4}$$

where u, v, ρ, and p have been obtained from the solution to Equations (2.12); Φ is given in Equation (2.6). The symbol ε is equal to zero for frozen flow (no vibrational relaxation), and one for nonequilibrium flow.

The coefficients A, B, C, F, and G are linear functions of U, V, R, and Ω:

$$\begin{aligned} A = &-\ M_\infty^{\,2}\ [\gamma/2 + (\gamma - 1)(u\dot{\rho} + \rho\dot{u})]\ U - (\gamma - 1)\ M_\infty^{\,2}\ (v\dot{\rho} + \rho\dot{v})\ V \\ &+ (\gamma - 1)(p\dot{\rho}/\rho^2)R \end{aligned} \tag{3.5}$$

$$B = (\dot{v}/v)\, U + [\dot{u}/v + (\zeta\dot{\rho})/(\rho^2 v) - 2\dot{v}g/v^2]\, V$$
$$+ (\zeta/\rho^2)(\dot{v}/v + 2\dot{\rho}/\rho)R$$

$$C = M_\infty^2\, (u - 2\gamma\zeta\dot{u} - \gamma\zeta/\rho)\, U + M_\infty^2\, (v - 2\gamma\zeta\dot{v})\, V \qquad (3.5)$$
$$+ (1/\rho^2)(p + 2\zeta\, \dot{p})R$$

$$F = \dot{\rho}\, \Omega + (1/\zeta)(\rho/2)(\Omega - \Phi/v)$$

$$G = pB + \zeta A/\rho - \varepsilon\, [\zeta\dot{\rho}\Omega/\rho + (1/2)(\Omega - \Phi/v)]$$

Equation (3.2) can be solved separately, using the initial condition, $\Omega(\zeta = 1) = 0$ (since E does not change along $\zeta = 1$); then Ω can be treated as a known function of ζ in Equations (3.3). Equations (3.3) are linear equations in U, V, and R, homogeneous when $\varepsilon = 0$ and non-homogeneous when $\varepsilon = 1$.

The pressure gradient function P_b is obtained by differentiating Equations (2.10) with respect to η and taking $\eta = \zeta = 0$:

$$P_b = -(\gamma M_\infty^2)\, \dot{\rho}_b\, (uU + vV)_b \qquad (3.6)$$

Initial conditions are applied at the shock wave and $\zeta = 1$; conditions there will be designated by the subscript w. For any function f

$$\partial f/\partial\eta\Big]_{\zeta = 1} = (\csc\beta)\, df/d\sigma = (\csc\beta)(df/d\beta)\, K_w$$

where σ is arc length along the shock wave and $K_w \equiv d\beta/d\sigma$ is the curvature of the shock. The initial conditions are

$$U_w = (du/d\beta)\, K_w \csc\beta, \qquad V_w = (dv/d\beta)\, K_w \csc\beta \qquad (3.7)$$
$$R_w = (d\rho/d\beta)\, K_w \csc\beta,$$

where $du/d\beta$, $dv/d\beta$, and $d\rho/d\beta$ are obtained by differentiating the shock relations; e.g., Equation (2.14).

The solution to Equations (3.3) can be written

$$U = K_w U_h + U_n, \qquad V = K_w V_h + V_n, \qquad R = K_w R_h + R_n \tag{3.8}$$

where U_h, V_h, and R_h are the solutions to the homogeneous equations, satisfying the initial conditions, Equation (3.7), with $K_w = 1$; U_n, V_n, and R_n are particular solutions to the non-homogeneous equations satisfying the initial conditions $(U_n)_w = (V_n)_w = (R_n)_w = 0$.

With the solutions U_h, U_n, ... R_n determined it remains to find K_w for the complete solution, Equation (3.8). This is found by applying the terminal condition, Equation (2.15) to the gradient functions. From Equation (2.15) one obtains

$$V_b = U_b \tan \theta_b + u_b \sec^2 \theta_b \, (\partial \theta_b / \partial \eta)_{\eta = 0} \tag{3.9}$$

also

$$(\partial \theta_b / \partial \eta)_{\eta = 0} = K_b \csc \theta_b \tag{3.10}$$

where $K_b \equiv d\theta_b/ds$ denotes the curvature of the body at the tip, and s the arc length along the body. Combining Equations (3.8), (3.9) and (3.10) gives the shock curvature in terms of the body curvature

$$K_w = \left[\frac{u \sec^2 \theta \csc \theta}{V_h - U_h \tan \theta}\right]_b K_b - \left[\frac{V_n - U_n \tan \theta}{V_h - U_h \tan \theta}\right]_b \tag{3.11}$$

Finally, the gradients on the body are given by

$$(dp/ds)_b = P_b \sin \theta_b, \qquad (dE/ds)_b = \Omega_b \sin \theta_b \tag{3.12}$$

$$(dT/ds)_b = (\rho P - pR)_b(\sin\theta_b)/\rho_b^2 \ ,$$

$$(dq/ds)_b = (uU + vV)_b(\sin\theta_b)/q_b \ , \qquad (3.12)$$

where P is given by Equation (3.6).

Equation (3.11) shows that the shock wave curvature at the tip of a pointed body of revolution is the sum of two terms; i) the curvature for a curved body in frozen flow, and ii) the curvature for nonequilibrium flow over a cone.

Previous calculations, Shen and Lin (1951), and Bianco et al. (1960), have been made of K_b/K_w for ideal gas flows ($\varepsilon = 0$ in Equations (3.3)). These and calculations from the present work indicate that K_b/K_w becomes zero for every axisymmetric body at some M_∞ which produces a partially subsonic, partially supersonic conical flow at the tip ($\eta = 0$). This implies that for each θ_b, there is an M_∞ for which, according to Equation (3.11),

$$(V_h - U_h \tan\theta)_b = 0.$$

This is the "Crocco point" in axisymmetric flow (see Ferri (1954)). It is also seen from Equation (3.11), that for these same values of M_∞ and θ_b the curvature of the shock wave in nonequilibrium flow becomes infinite at the tip of the cone (where $K_b = 0$).

4. SOLUTION IN THE VICINITY OF THE SINGULAR POINT

The equations for the gradient functions (3.2) and (3.3) have a regular singular point at $\zeta = 0$. Following Ince (1926) the first step in examining the nature of the solutions in the neighborhood of the singular point is to set up the indicial equation and find its roots. When this is done for Equations (3.2) and (3.3) it is found that the

roots are: 0, 0, 1/2, 1/2. The presence of the two double roots indicate that logarithmic terms must be included. Thus, each variable has the form

$$P_1 + (\log \zeta)\, P_2 + \zeta^{1/2}\, P_3 + (\zeta^{1/2} \log \zeta)\, P_4 \qquad (4.1)$$

where the P_i denotes power series with unknown coefficients. Recurrence relations obtained by substituting these forms into the differential equations determine the coefficients of the power series in terms of the arbitrary constants.

Since a numerical solution to Equations (3.2) and (3.3) is obtained, a lengthy discussion of the singularity is not needed. Suffice it to say that the constant terms in the series P_2 and P_4 are zero for each variable. Thus, each gradient function has the form

$$\text{constant} + (\zeta^{1/2} \times \text{constant}) \qquad (4.2)$$

in the neighborhood of $\zeta = 0$.

5. NUMERICAL SOLUTION

Equations (2.12) are first solved separately; then Equations (3.2) and (3.3) are solved. The Runge-Kutta-Gill method is used to integrate the equations numerically.

With high speed computers it is possible to study the solution empirically by carrying out a "detailed approach" to the body; that is, to systematically decrease the interval size in the Runge-Kutta-Gill procedure as ζ approaches zero, ending the calculation at an extremely small but finite value of $\zeta(\sim 10^{-12})$. This is the method used in the present work. While admittedly not elegant, this procedure does produce answers in reasonably short times, and *a posteriori* tests indicate that the values obtained are correct. Thus, unique limits for the gradient

functions are found as the integration interval and limiting ζ approach zero; also, the calculated gradient functions exhibit the $\zeta^{1/2}$ variation near zero, Equation (4.2), which was demonstrated in Section 4. In addition, the calculated solution to Equation (3.2) agrees with the known value ($\Omega = \Phi/v$) obtained from Taylor-Maccoll flow.

6. RESULTS

In the case of cones (where $K_b = 0$) the shock curvature K_w reduces to the second term of the expression in Equation (3.11). This quantity was calculated for a wide range of Mach numbers and cone angles for nitrogen at 300°K. Results are shown in Figure 3 (solid curves). Each curve has a vertical asymptote occurring at a cone angle for which the Taylor-Maccoll flow is supersonic at the shock wave, but subsonic at the body; K_w changes sign here and then decreases in absolute value with increasing θ_b. The qualitative behavior of K_w is similar to that of shock curvature at a wedge tip, shown also in Figure 3. Figure 4 shows the variation of the pressure gradient at the tip of a cone; the "Crocco point" asymptotes appear here also.

From results of Millikan and White (1963) some representative values of $\tau_b' q_\infty'$, the normalizing quantity for distances, are: $\tau_b' q_\infty' = 5.2$, 0.26, and 0.034 cm for $\theta_b = 30°$, 40°, and 50°, respectively, at $M_\infty = 10$, $p_\infty' = 1$ atmosphere; for other p_∞', the given $\tau_b' q_\infty'$ is to be divided by the number of atmospheres.

In Figure 5 the gradients of pressure, temperature, and density at the tip of a cone are given as functions of cone angle for $M_\infty = 10$, $T_\infty' = 300°K$ in nitrogen. The density gradient is unusual in that it is non-monotonic and changes sign; this change in sign takes place when the flow on the cone surface is subsonic. A similar type variation is found for density gradient at the tip of a wedge and is indicated in this figure; here the change in sign occurs for supersonic flow at the

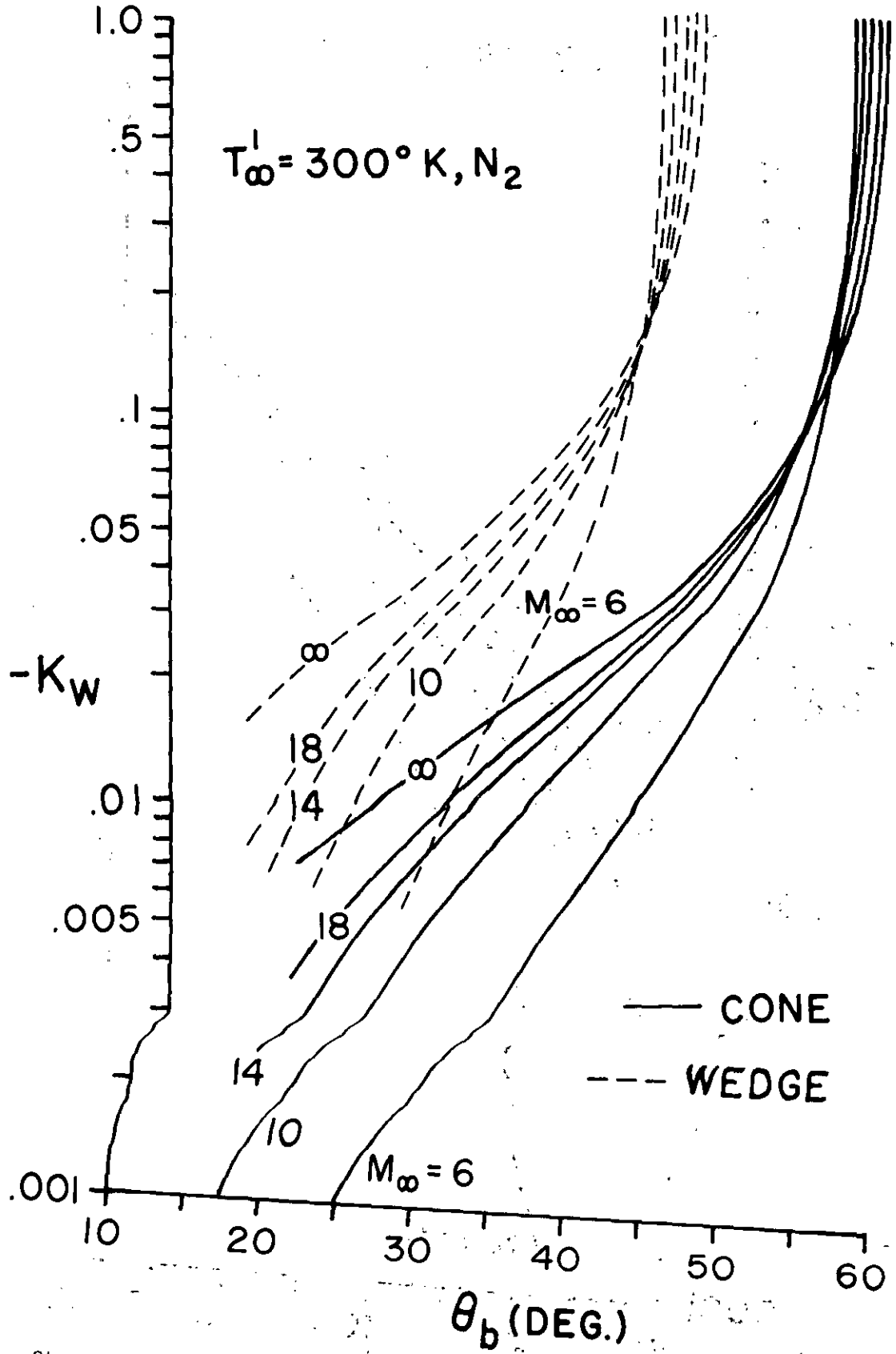

Figure 3. Shock wave curvature at the tip of pointed body vs. body half-angle.

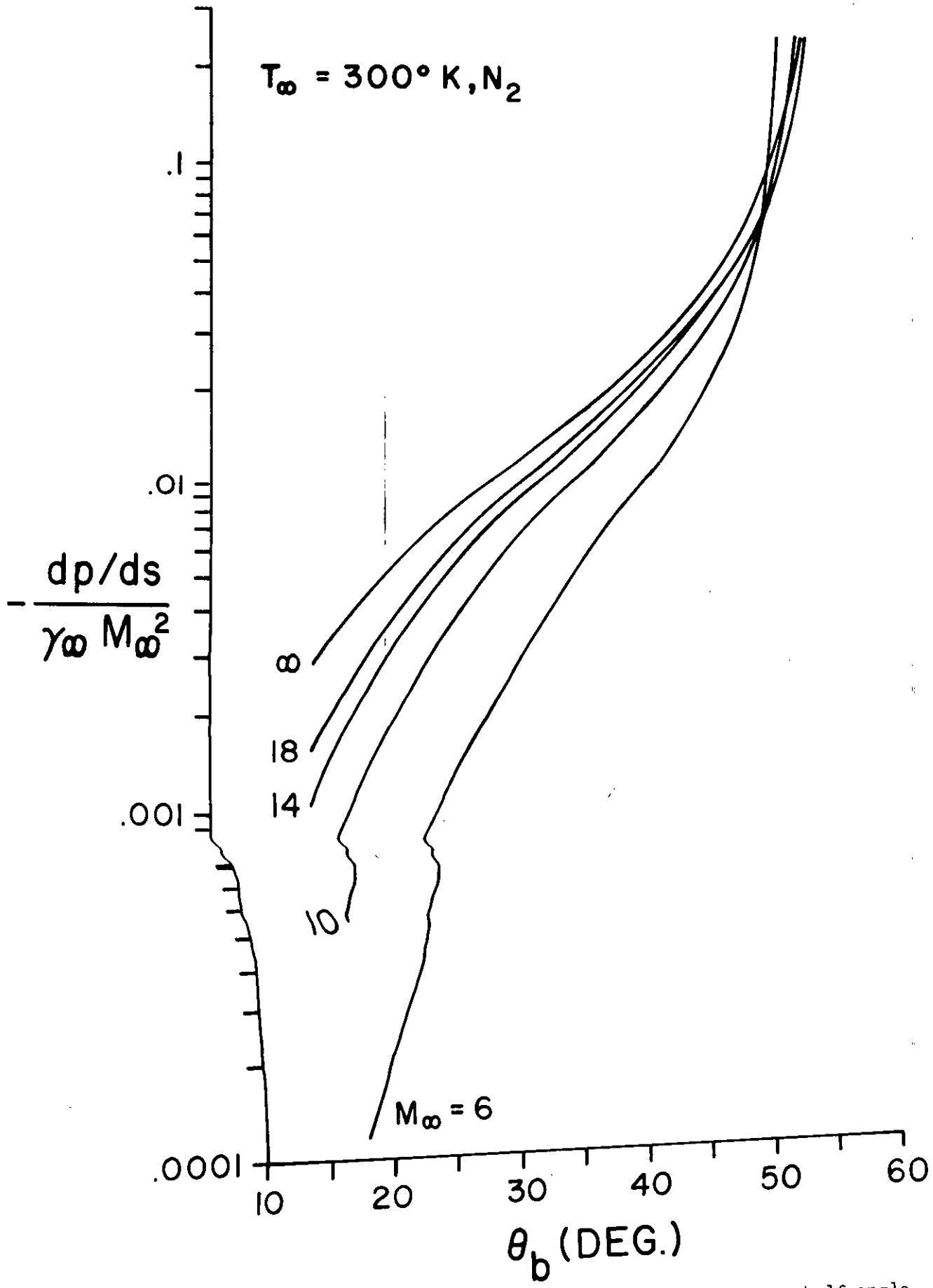

Figure 4. Pressure gradient along body at tip of cone vs. cone half-angle.

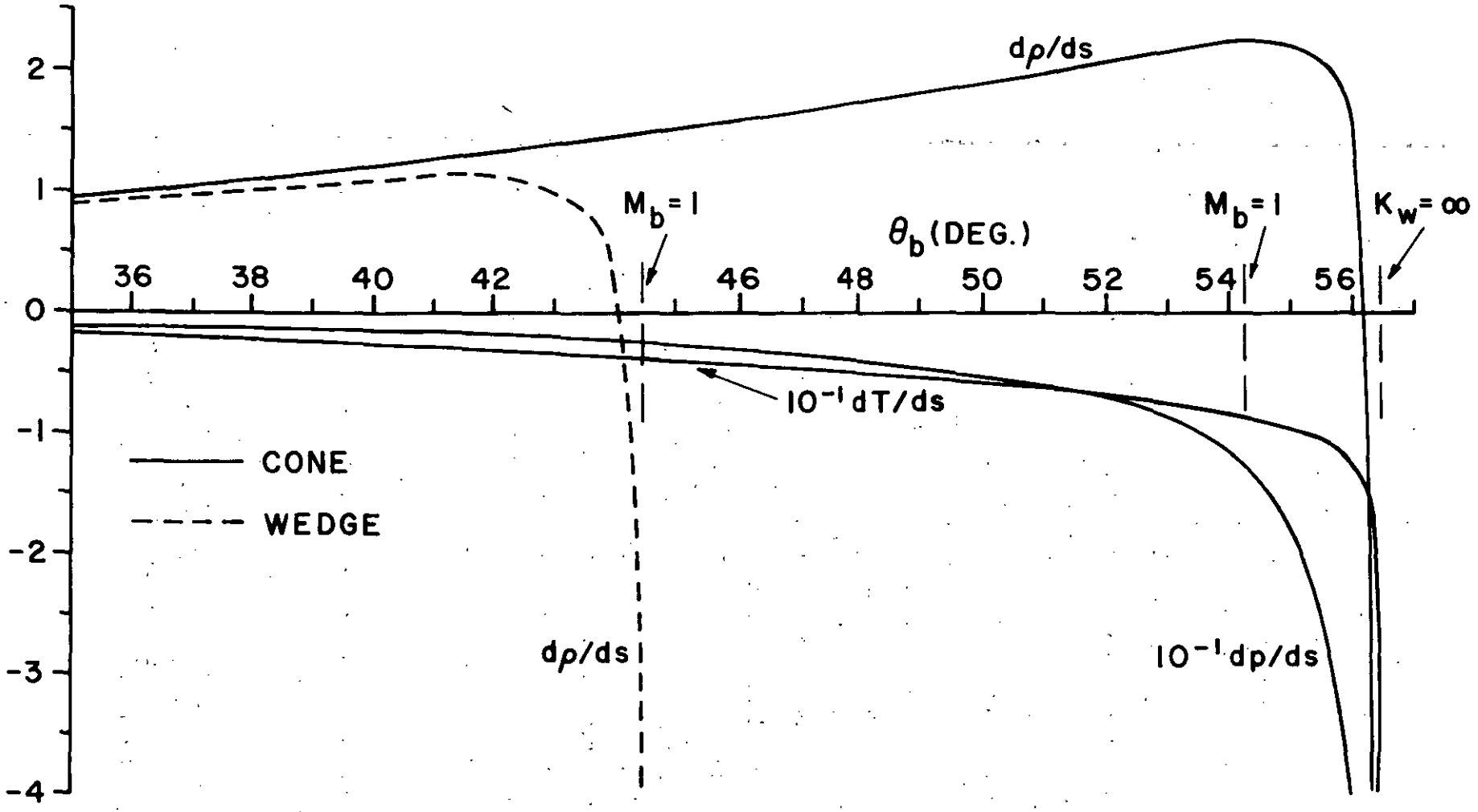

Figure 5. Flow variable gradients at tip of pointed body vs. body half-angle N_2 gas, $T_\infty' = 300^0K$, $M_\infty = 10$.

wedge surface. Similar behavior for the density gradient in plane flow was found for the case of dissociating air,* using the gas model and gradient formulae of Spurk, et al. (1966).

As mentioned in Section 1, the present work has application in the calculation of axisymmetric nonequilibrium flows. In previous work, Sedney and Gerber (1963), an initial region of frozen flow was assumed in order to start a nonequilibrium flow computation by the method of characteristics. This lead to results illustrated in Figure 6 for pressure variation on the body in a typical case of flow over a cone. The results are clearly in error near the tip; however, a curve drawn through the points further downstream can be faired back easily to the correct pressure at the tip, as evidenced by the solid curve. This furnishes an indication that the results downstream are correct. The gradient calculations, indicated by the dashed lines, give further assurance of the validity of the characteristic computations downstream by demonstrating that the solid curves can be extended back to the tip pressure with the correct slope. Gradient values can also be useful in initiating nonequilibrium characteristic flow computations.

The present results can be compared with those obtained by an application of Dorodnitsyn's integral method, South and Newman (1965). This latter procedure is an approximate method which yields algebraic equations for the curvature and gradients at the tip of a cone. Figure 7 shows the comparison for two Mach numbers. The agreement, in general, is good; it is found to improve as the angle interval $\beta - \theta_b$ decreases.

7. CONCLUSION

A method is given for determining the shock curvature and flow variable gradients at the tip of a pointed body of revolution. The use of variables introduced by Chester simplifies setting up the calculations

---

* *A characteristic calculation of one example with an initially negative density gradient was performed. The gradient changed sign at a distance of 3x (initial frozen length) and thereafter was positive. All other flow variables were monotonic.*

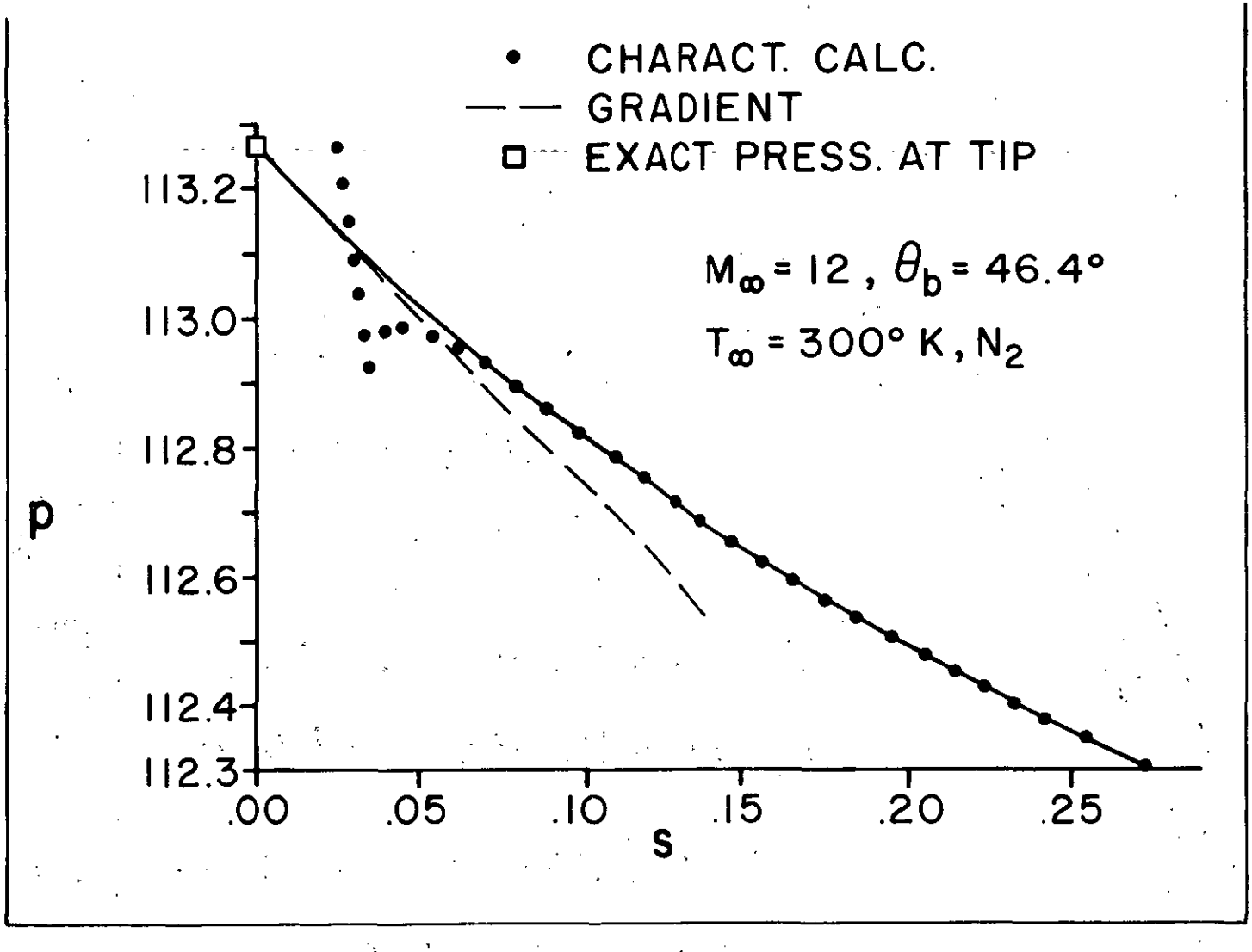

Figure 6. Application of pressure gradient calculations to check characteristic calculations.

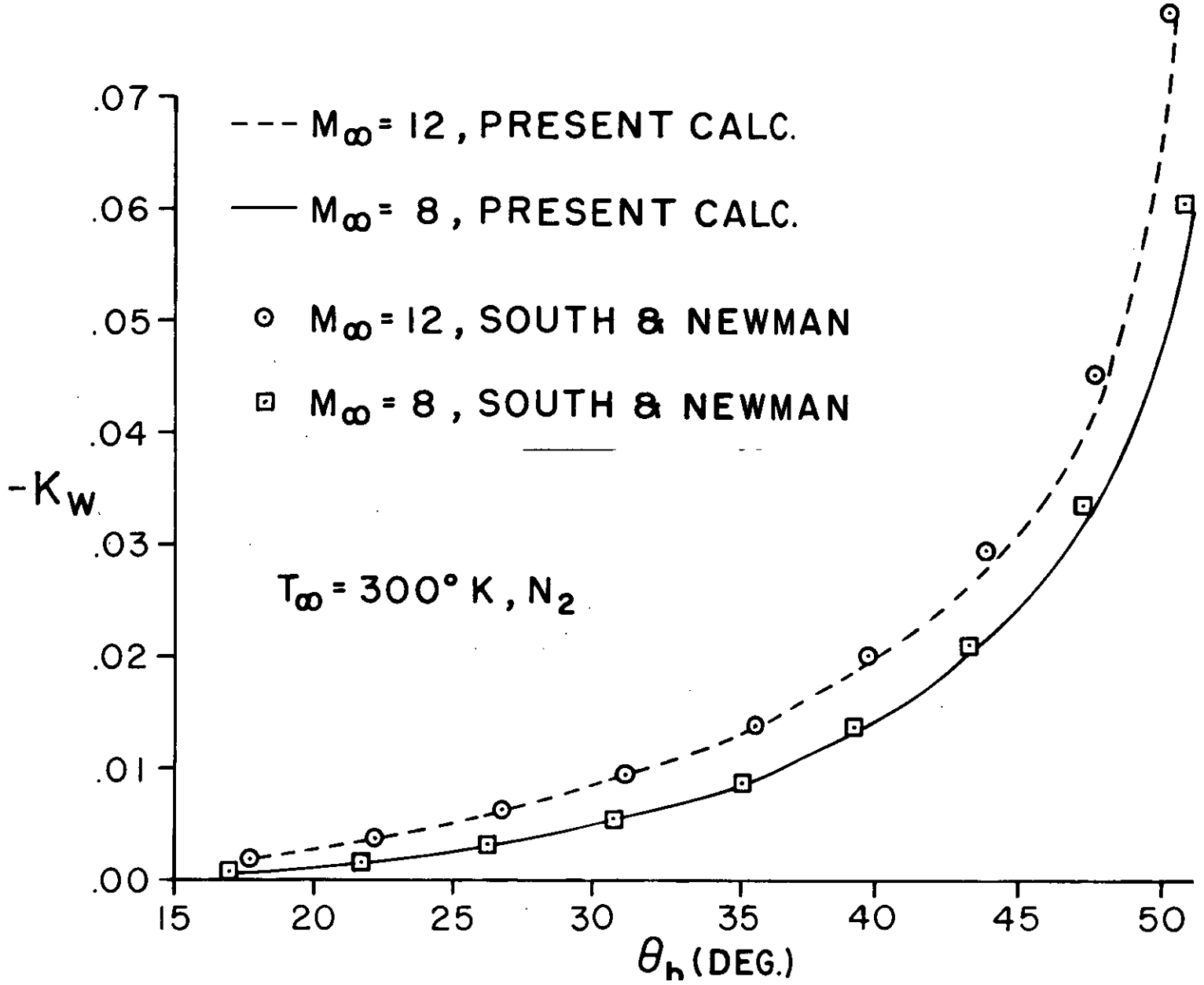

Figure 7. Comparison of present calculations of shock wave curvature with integral method calculations of South and Newman.

as compared to use of polar coordinates. Although the specific source of departure from equilibrium considered here is vibrational excitation, the same technique can be applied to a dissociating gas, with the same qualitative results expected.

It is shown that the shock curvature at the tip of a pointed body of revolution is the sum of two terms: i) the curvature for a curved body in frozen flow and ii) the curvature for nonequilibrium flow over a cone. Also, the Crocco point for nonequilibrium flow occurs at the same Mach number and cone angle combination as for frozen flow.

ACKNOWLEDGEMENTS

The authors wish to acknowledge here the programming and computing work of Donald Taylor and Lynn Bartlett, and the assistance of Joan M. Bartos and Gerald Nathe.

R. SEDNEY N. GERBER

BIBLIOGRAPHY

1. Bianco, E; Cabannes, H. and Kuntzmann, J. Curvature of Attached Shock Waves in Steady Axially Symmetric Flow. J. Fluid Mech., 7, 610-616, 1960.

2. Blackman, V. Vibrational Relaxation in Oxygen and Nitrogen. J. Fluid Mech., 1, 61, 1956.

3. Chester, W. Supersonic Flow Past a Bluff Body with a Detached Shock, Part II, Axisymmetric Body. J. Fluid Mech., 1, 490-496, 1956.

4. Crocco, L. Singolarita Della Corrente Gassosa Iperacustica Nell' Intorno Di Una Prora a Diedro. L'Aerotecnica, t. XVII, Fasc. 6, 519-534, 1937.

5. Ferri, A. Article in High Speed Aerodynamics and Jet Propulsion. Vol. VI (p. 678) W. Sears, Editor. Princeton University Press, Princeton, New Jersey, 1954.

6. Ince, E. L. Ordinary Differential Equations. Dover Publications 1944, New York, New York 1926.

7. Kogan, A. On Supersonic Rotational Flow Behind Strong Shock Waves, II. Flow Past Ogives of Revolution. Technical Report, Technion Research and Development Foundation, Ltd., Haifa, Israel, 1956.

8. Millikan, R. C. and White, D. R. Vibrational Energy Exchange Between N_2 and CO. The Vibrational Relaxation of Nitrogen. J. Chem. Phys., 39, 98-101, 1963.

9. Sedney, R. Some Aspects of Nonequilibrium Flows. J. Aerospace Sci., 28, 189-197, 1961.

10. Sedney, R. and Gerber, N. Nonequilibrium Flow Over a Cone. AIAA Jour., 1, 2482-2486, 1963.

11. Shen, S. F. and Lin, C. C. On the Attached Curved Shock in Front of a Sharp-Nosed Axially Symmetrical Body Placed in a Uniform Stream. N.A.C.A. Technical Note 2505, 1951.

12. South, J. C., Jr. and Newman, P. A. Application of the Method of Integral Relations to Real-Gas Flows Past Pointed Bodies. AIAA Jour., 3, 1645-1652, 1965.

13. Spurk, J. H., Gerber, N. and Sedney, R. Characteristic Calculation of Flowfields with Chemical Reactions. AIAA Jour., 4, 30-37, 1966.

DISTRIBUTION LIST

No. of Copies	Organization
20	Commander Defense Documentation Center ATTN: TIPCR Cameron Station Alexandria, Virginia 22314
1	Commanding General U.S. Army Materiel Command ATTN: AMCRD-TP Washington, D.C. 20315
2	Commanding General U.S. Army Missile Command ATTN: AMSMI-AML Redstone Arsenal, Alabama 35809
1	Commanding Officer U.S. Army Engineer Research & Development Laboratories ATTN: STINFO Div Fort Belvoir, Virginia 22060
1	Commanding General U.S. Army White Sands Missile Range White Sands Missile Range New Mexico 88002
1	Director U.S. Army Research Office 3045 Columbia Pike Arlington, Virginia 22204
3	Commander U.S. Naval Air Systems Command Headquarters ATTN: AIR-604 Washington, D.C. 20360
2	Commander U.S. Naval Ordnance Laboratory ATTN: Lib Silver Spring, Maryland 20910
1	Commander U.S. Naval Ordnance Test Station ATTN: Code 753 China Lake, California 93557
2	Superintendent U.S. Naval Postgraduate School ATTN: Tech Rept Sec Monterey, California 93940
1	Commander U.S. Naval Weapons Laboratory ATTN: Lib Dahlgren, Virginia 22448
1	AEDC (AER) Arnold AFS Tennessee 37389
1	RTD (RTTM) Bolling AFB, D.C. 20332
1	APGC (PGBPS-12) Eglin AFB Florida 32542
1	AUL (3T-AUL-60-118) Maxwell AFB Alabama 36112
1	AFFDL (FDM) Wright-Patterson AFB Ohio 45433
1	Director Los Alamos Scientific Laboratory University of California P.O. Box 1663 Los Alamos, New Mexico 87544

DISTRIBUTION LIST

No. of Copies	Organization
1	Director NASA Scientific and Technical Information Facility ATTN: SAK/DL P.O. Box 33 College Park, Maryland 20740
2	Director National Aeronautics and Space Administration Ames Research Center ATTN: Mr. H. Allen Mr. A. Seiff Moffett Field, California 94035
1	Director Jet Propulsion Laboratory 4800 Oak Grove Drive Pasadena, California 91103
3	Director National Aeronautics and Space Administration Langley Research Center ATTN: Mr. J. South Mr. R. Trimpi Langley Station Hampton, Virginia 23365
1	Director National Aeronautics and Space Administration Lewis Research Center 21000 Brookpark Road Cleveland, Ohio 44135
1	Director Applied Physics Laboratory The Johns Hopkins University 8621 Georgia Avenue Silver Spring, Maryland 20910
1	Aerospace Corporation ATTN: Mr. Z. Bleviss P.O. Box 95085 Los Angeles, California 90045
1	Sandia Corporation Livermore Laboratory ATTN: Tech Lib P.O. Box 969 Livermore, California 94550
1	Cornell Aeronautical Laboratory Inc. ATTN: Mr. J. G. Hall P.O. Box 235 Buffalo, New York 14221
2	IIT Research Institute ATTN: Mr. D. Hacker Mr. P. Chiarulli 10 West 35th Street Chicago, Illinois 60616
1	Massachusetts Institute of Technology ATTN: Mr. J. Baron 77 Massachusetts Avenue Cambridge, Massachusetts 02139
1	Polytechnic Institute of Brooklyn ATTN: Dean M. Bloom Route 110 Farmingdale, New York 11735
2	Rensselaer Polytechnic Institute ATTN: Mr. T. Li Mr. G. Handelman Troy, New York 12181
1	Stanford University ATTN: Mr. M. VanDyke Stanford, California 94305

DISTRIBUTION LIST

No. of Copies	Organization
1	University of Illinois Aeronautical Institute Urbana, Illinois 61803
1	University of Southern California ATTN: Dir, Engr Ctr 3551 University Avenue Los Angeles, California 90007
1	Yale University Mason Laboratory ATTN: Mr. W. Klikoff 400 Temple Street New Haven, Connecticut 06510
1	Professor S. Bogdonoff Forrestal Research Center Princeton University Princeton, New Jersey 08540
1	Professor G. Carrier Division of Engineering and Applied Physics Harvard University Cambridge, Massachusetts 01238
1	Professor F. Clauser University of California Santa Cruz, California 95060
1	Professor H. Emmons Harvard University Cambridge, Massachusetts 01238
1	Professor W. Haynes Forrestal Research Center Princeton University Princeton, New Jersey 08540
1	Professor L. Lees Guggenheim Aeronautical Laboratory California Institute of Technology Pasadena, California 91004
1	Professor H. Liepmann Aeronautics Department California Institute of Technology 1201 East California Blvd Pasadena, California 91102
1	Professor S. I. Pai Institute of Fluid Dynamics & Applied Mathematics University of Maryland College Park, Maryland 20740
1	Professor R. Probstein Massachusetts Institute of Technology 77 Massachusetts Avenue Cambridge, Massachusetts 02139
1	Dr. A. Charters Defense Research Laboratories General Motors Corporation Santa Barbara, California 93108
1	Dr. J. Clark Division of Applied Mathematics Brown University Providence, Rhode Island 02912
1	Dr. S. Maslin Research Institute for Advanced Studies The Martin Company 7212 Bellona Avenue Ruxton, Maryland 21212

DISTRIBUTION LIST

No. of Copies	Organization
1	Dr. A. Puckett Systems Development Laboratory Hughes Aircraft Company Florence Avenue & Teal Street Culver City, California 90232
1	Dr. W. Sears Graduate School of Aeronautical Engineering Cornell University Ithaca, New York 14850
1	Dr. R. Sedney Research Institute for Advanced Studies The Martin Company 7212 Bellona Avenue Ruxton, Maryland 21212
1	Dr. J. Sternberg The Martin Company Baltimore, Maryland 21203
1	Dr. J. Lukasiewicz Von Karman Gas Dynamics Facility ARO, Incorporated Arnold AFS, Tennessee 37389
1	Mr. H. Nagamatsu General Electric Research Laboratory P.O. Box 1088 Schenectady, New York 13205
1	Mr. P. Rose AVCO-Everett Research Laboratory 2385 Revere Beach Parkway Everett, Massachusetts 02149
1	Mr. J. Whitfield Von Karman Gas Dynamics Facility ARO, Incorporated Arnold AFS, Tennessee 37389
1	Mr. H. Yoshihara General Dynamics/CONVAIR P.O. Box 1950 San Diego, California 92112
	Aberdeen Proving Ground
	Ch, Tech Lib Air Force Ln Ofc Marine Corps Ln Ofc Navy Ln Ofc CDC Ln Ofc